Nonequilibrium transport through a singlet-triplet Anderson impurity

P. Roura Bas*
Centro Atómico Constituyentes, Comisión Nacional de Energía Atómica, 1650 San Martín, Buenos Aires, Argentina

A. A. Aligia
Centro Atómico Bariloche and Instituto Balseiro, Comisión Nacional de Energía Atómica, 8400 Bariloche, Argentina

(Received 17 June 2009; published 13 July 2009)

We study the Anderson model in which a configuration with a doublet is hybridized with another with a singlet and a triplet. We calculate the conductance through the system as a function of temperature and bias voltage near the quantum critical line for which the system is exactly solvable. The results explain recent transport measurements in a single-molecule quantum dot.

DOI: 10.1103/PhysRevB.80.035308 PACS number(s): 73.63.Kv, 72.15.Qm, 73.23.Hk, 75.20.Hr

I. INTRODUCTION

When the wave function is forced to evolve continuously between two competing ground states, a quantum phase transition (QPT) takes place between these two states At the transition, the length scale of quantum fluctuations becomes infinite and exotic states of condensed matter are expected.[1] Recently, several remarkable features of a QPT have been observed in C_{60} quantum dots (QD's) with even occupancy inserted in a nanoscale constriction.[2] In the last few years there has been a great interest in systems of quantum dots because of the possible technological applications and also because they constitute ideal systems with a single magnetic impurity in which several parameters can be tuned.

When the QD has an odd number of electrons and the Coulomb repulsion U is large enough, the conductance at zero bias is increased below a characteristic Kondo temperature T_K as a consequence of the Kondo effect. This is a usual feature of single-electron transistors built with semiconductor QD's or single molecules[3,4] and is well understood in terms of the simplest ordinary Anderson model (OAM) in which a configuration with a doublet is hybridized with a singlet. In a dot with an even number of electrons, there are two competing states for the ground-state configuration: a singlet in which two particles occupy the lowest level (say $|00\rangle = s_\uparrow^\dagger s_\downarrow^\dagger |0\rangle$) and a triplet in which one electron is promoted to the next level and coupled ferromagnetically [$|11\rangle = p_\uparrow^\dagger s_\uparrow^\dagger |0\rangle$ and its SU(2) partners] due to the strong Hund coupling.[5] The simplest Anderson model which describes the system mixes these four states with a doublet ($|\sigma\rangle = s_\sigma^\dagger |0\rangle$) by promoting a particle (electron or hole) to one of the leads.[6,7] This is the singlet-triplet Anderson model (STAM) which had been used to describe valence fluctuating Tm impurities in a cubic environment.[8]

This model has a quantum phase transition from a singlet to a doublet ground state as the energy of the triplet is decreased.[6,8] When the triplet is well below the other states, there is a partial screening of the spin 1 that explains the zero-bias Kondo peak observed experimentally in this situation.[9,10] On the other (singlet) side of the transition, there is a dip in the conductance[6,7] that has also been observed experimentally.[2,7]

In this paper, we show that the experimental observations in C_{60} QD's can be understood in terms of this model and its QPT. The differential conductance dI/dV as a function of temperature T and bias voltage V has been measured at both sides of the transition.[2] On the singlet side of the transition, a dip in the conductance at $V=0$ is observed in agreement with theoretical expectations[6,7] as well as nonequilibrium measurements performed in carbon nanotubes.[7] On the other side of the transition, dI/dV as a function of V shows a structure with three peaks that has not been quantitatively explained yet. As the temperature T is decreased, the zero-bias conductance $G(T)$ first increases then shows a shoulder or a plateau and then increases again. As stressed by the authors, this behavior is still not understood.[2] The last two figures of our paper are the theoretical counterparts of these experimental results. The main qualitative features are reproduced. A more quantitative agreement would require a fine tuning of the parameters which is beyond the scope of this paper. We provide an interpretation for the observed behavior.

II. THE MODEL

The STAM assumes infinite U and contains two neighboring charge configurations in the QD: d^n and d^{n+1} with n and $n+1$ particles. Without loss of generality we can assume n to be even, performing an electron-hole transformation if necessary. Then the d^n configuration contains a singlet $|SM\rangle = |00\rangle$, where S is the spin and M its projection, and a triplet $|1M\rangle$, ($M=-1$, 0 or 1), while the d^{n+1} configuration consists of a doublet denoted by its spin 1/2 projection $|\sigma\rangle$. We introduce the following creation operators for a particle in the dot[11]

$$d_{s\sigma}^\dagger = |\sigma\rangle\langle 00|,$$

$$d_{t\uparrow}^\dagger = -(|\uparrow\rangle\langle 10| + \sqrt{2}|\downarrow\rangle\langle 1-1|)/\sqrt{3},$$

$$d_{t\downarrow}^\dagger = (|\downarrow\rangle\langle 10| + \sqrt{2}|\uparrow\rangle\langle 11|)/\sqrt{3}. \quad (1)$$

The operators $d_{s\sigma}^\dagger$ and $d_{t\sigma}^\dagger$ hybridize via matrix elements $V_{\nu k}^s$ and $V_{\nu k}^t$ with the conduction states $c_{\nu k\sigma}$ of two conducting leads $\nu=L$ (left) or R (right) that transport the current through the QD, leading to the Hamiltonian

$$H = E_s|00\rangle\langle 00| + E_t\sum_M |1M\rangle\langle 1M| + E_d\sum_\sigma |\sigma\rangle\langle\sigma| + \sum_{\nu k\sigma}[(V^s_{\nu k}d^\dagger_{s\sigma} + V^t_{\nu k}d^\dagger_{t\sigma})c_{\nu k\sigma} + \text{H.c.}] + \sum_{\nu k\sigma}\epsilon_{\nu k}c^\dagger_{\nu k\sigma}c_{\nu k\sigma}. \quad (2)$$

We assume $V^s_{Lk}V^t_{Rk}=V^t_{Lk}V^s_{Rk}$, so that only one conduction channel $\sim\Sigma_{\nu k\sigma}V^\eta_{\nu k}c_{\nu k\sigma}$ ($\eta=s$ or t) hybridizes with the dot states. In general, also the orthogonal linear combination of $c_{\nu k\sigma}$ plays a role and "screens" the remaining doublet ground state when the localized triplet is well below the singlet, leading to a singlet ground state.[12,13] However, the energy scale involved in this second screening T^* (which depends exponentially on a small coupling constant[13]) might be very small. As discussed in Ref. 13, this is likely the case of previous experiments,[9,10] as well as those in C_{60} QD's:[2] the theory in the general case[12,13] predicts that the zero-bias conductance $G(T)$ should decrease at very low temperatures and dI/dV should also decrease for the smallest applied bias voltages V in contrast to the observations. This indicates that T^* is smaller than the smallest temperature in the experiments.

The STAM with only one conduction channel also describes the mixing between the low-lying states of the $4f^{12}$ and $4f^{13}$ configurations in a cubic crystal field.[8] For $E_t\to+\infty$, the model reduces to the OAM. For $E_s\to+\infty$, the model describes valence fluctuations between two magnetic configurations.[14] In both limits, for constant density of conduction states and hybridizations, the model is exactly solvable (by the Bethe ansatz) and the ground state is a singlet (doublet) in the first (second) case.[14] Thus, the model has a QPT as a function of E_s-E_t. The position of the transition depends on the other parameters of the model, leading to a quantum critical surface that can be determined by calculating the magnetic susceptibility at $T\to 0$ using numerical renormalization group (NRG).[8] However, if $|V_t|^2=3|V_s|^2$, the transition takes place exactly at $E_s-E_t=0$, independently of the value of E_d. In addition, along this line, the model can be mapped into an OAM plus a free spin 1/2.[8] We will use these results to control the distance to the QCP.

III. APPROXIMATIONS AND EQUATION FOR THE CURRENT

As discussed for example in Ref. 15 the calculation of nonequilibrium properties of a strongly correlated system is a particular challenge for theory. A recent extension of the numerical renormalization group for the nonequilibrium case seems promising but is not fully developed yet.[16] For the OAM, the noncrossing approximation (NCA) (Ref. 17) and renormalized perturbation theory in U (Refs 18 and 19) have been useful. However, the latter is very difficult to extend to the STAM. The so-called poor man's scaling works well when either eV or the magnetic field energy is larger than kT_K (Ref. 20) and has been successfully extended for a model similar to the STAM on the singlet side of the QPT.[7] However, this method ceases to be valid near the quantum critical surface for small V. Instead, the NCA can be extended to more general Anderson models, like those appropriate for Ce compounds,[21] Co impurities on Ag and Cu,[22] or systems of two quantum dots out of equilibrium.[23]

In this paper, we extend the NCA to the STAM out of equilibrium. We introduce auxiliary bosons, one for the singlet state and three for the triplets, and auxiliary fermions for the doublet, in analogy to the $SU(N)\times SU(M)$ generalization of the Anderson model.[24] The spectral densities of the operators $d^\dagger_{\eta\sigma}$ defined by Eq. (1) for the given spins $\rho^s_d(\omega)$ and $\rho^t_d(\omega)$ are determined by convolutions from those of the auxiliary particles. The current is given by[25]

$$I = \frac{A\pi e}{h}\int d\omega[\Gamma^s\rho^s_d(\omega)+\Gamma^t\rho^t_d(\omega)][f_L(\omega)-f_R(\omega)], \quad (3)$$

where $\Gamma^\eta=\Gamma^\eta_R+\Gamma^\eta_L$ with $\Gamma^\eta_\nu=2\pi\Sigma_k|V^\eta_{\nu k}|^2\delta(\omega-\epsilon_k)$ are assumed to be independent of ω within a bandwidth D and zero elsewhere, the asymmetry parameter is $A=4\Gamma^\eta_R\Gamma^\eta_L/(\Gamma^\eta_R+\Gamma^\eta_L)^2$ (independent of η), and $f_\nu(\omega)$ is the Fermi function with the chemical potential μ_ν of the corresponding lead.

IV. RESULTS

For the numerical evaluations, we consider the case in which the ground-state configuration has an even number of particles ($E_s,E_t<E_d$). We choose $E_d=(\mu_L+\mu_R)=0$ (without loss of generality) and take a bandwidth $D=10\Gamma$, $\Gamma^s=1/2\Gamma$ and $\Gamma^t=3/2\Gamma$, where Γ is the unit of energy. The choice $\Gamma^t/\Gamma^s=3$ allows us to have an accurate control of the distance to the QPT, while the main features of the results depend on this distance and not on the specific choice of parameters. For $\Gamma^t/\Gamma^s=3$, if in addition $E_s=E_t$, the STAM can be mapped into an OAM plus a free spin 1/2 (Ref. 8). The OAM has total coupling $\Gamma^{\text{OAM}}=\Gamma$ and inverted charge-transfer energy and chemical potentials $E^{\text{OAM}}_d-E^{\text{OAM}}_s=E_s-E_d$ and $\mu^{\text{OAM}}_\nu=-\mu_\nu$. Using this mapping it can be shown that the densities of both models are related by $\rho^s_d(\omega)=\rho^t_d(\omega)=\rho^{\text{OAM}}_d(-\omega)/2$ and the absolute value of current is the same. From the structure of the corresponding NCA equations for both models, we realize that the NCA satisfies these equalities. This has also been verified numerically. Furthermore, for any E_d the QPT takes place at $E_s=E_t$, when $\Gamma^t/\Gamma^s=3$.[8] This defines a quantum critical line and then E_s-E_t controls the distance to this line.

As explained above, for $V=0$ ($\mu_L=\mu_R=0$), when $E_s=E_t$, the singlet and triplet parts of the spectral density of the dot $2\rho^s_d(\omega)$ and $2\rho^t_d(\omega)$ coincide with the mirror image of the localized spectral density already reported for the Anderson model (Fig. 5 of Ref. 17 for $E_t=-2\Gamma$) and exhibit the usual Kondo resonance at the Fermi level. The half width of this peak allows to define a Kondo temperature T_K. How do the spectral densities evolve as one moves away from the quantum critical surface? Decreasing E_s (on the singlet side of the QPT) $\rho^s_d(\omega)$ displaces to positive frequencies, while $\rho^t_d(\omega)$ decreases and displaces its weight to negative frequencies. As a consequence, a gap opens in the sum $\Gamma^s\rho^s_d(\omega)+\Gamma^t\rho^t_d(\omega)$ entering Eq. (3) at low temperatures. This situation has already been studied previously and interpreted as the low-temperature part of a two-stage Kondo effect.[6]

The spectral densities for $E_s>E_t$ are shown in Fig. 1. In contrast to the previous case, $\rho^t_d(\omega)$ remains peaked at the

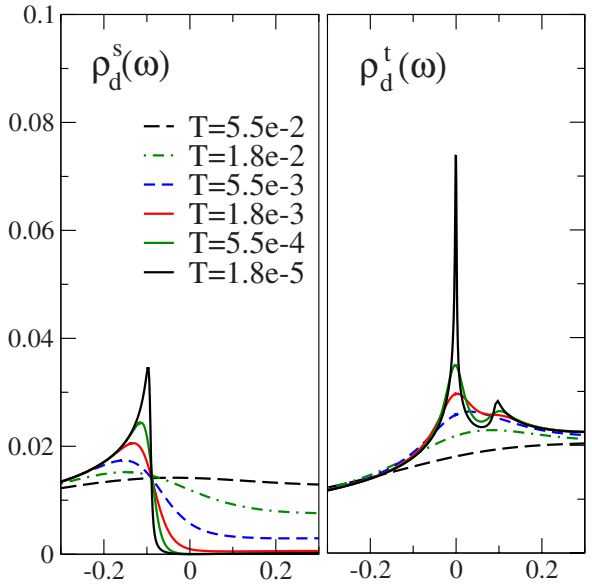

FIG. 1. (Color online) Singlet (left) and triplet (right) contributions to the dot spectral density for $E_t=-3, E_s=-2.9$ and different temperatures. The flatter curve corresponds to the highest temperature. Γ is the unit of energy.

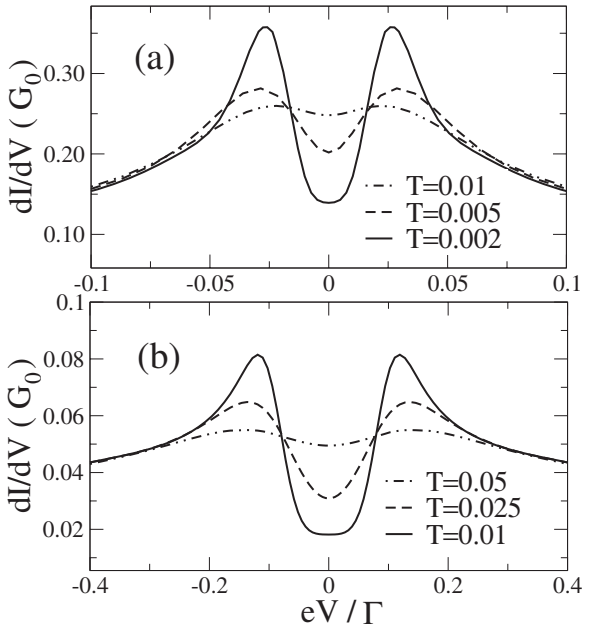

FIG. 2. Differential conductance as a function of bias voltage for several temperatures. (a) $E_t=-2, E_s=-2.03$ and (b) $E_t=-3, E_s=-3.1$.

Fermi energy at low temperatures. This is a consequence of the partial Kondo effect, by which the spin 1 at the dot forms a ground-state doublet with the conduction electrons of both leads.[14] The singlet part of the density $\rho_d^s(\omega)$ displaces to negative frequencies in this case. Therefore a pseudogap appears in the sum, $\Gamma^s\rho_d^s(\omega)+\Gamma^t\rho_d^t(\omega)$, but at finite frequencies, in contrast to the gap at the Fermi level that develops at the singlet side of the QPT. Note that at high temperatures both densities are quite similar and the differentiation between $\rho_d^s(\omega)$ and $\rho_d^t(\omega)$ develops at a characteristic temperature on the order of a fraction of E_s-E_t.

The equilibrium ($V=0$) conductance as a function of temperature $G(T)$ on the singlet side of the QPT near the quantum critical line (not shown) shows a maximum at a finite temperature and agrees with previous results using NRG (Ref. 6) and with experiment.[2] In particular, the increase and decrease in $G(T)$ from its maximum value are logarithmic to a good degree of accuracy.

The differential conductance dI/dV as a function of bias voltage on the singlet side of the transition is displayed in Fig. 2(a). We have applied the voltage symmetrically ($\mu_L=-\mu_R=eV/2$). As the temperature is lowered, a dip develops at small voltages. The half width of the dip is on the order of E_t-E_s. These results are in good agreement with the experimental ones (Fig. 4c of Ref. 2). For other parameters, in particular larger values of E_t-E_s and E_d-E_s (less valence fluctuations), we obtain curves that look similar to those reported in carbon nanotubes with a flat bottom at low temperatures, explained using poor man's scaling.[7] An example is illustrated in Fig. 2(b)

The most distinct experimental results are those on the "triplet side" of the transition ($E_s>E_t$). As the temperature is decreased, $G(T)$ increases until it reaches a plateau at the characteristic energy E_s-E_t and then it continues to increase.[2] This is in general, the behavior that we obtain, as displayed in Fig. 3. As the partial contribution to the conductance for each density reveals, the plateau is due to the contribution of the singlet part of the dot spectral density, namely $\rho_d^s(\omega)$, which is peaked at $-(E_s-E_t)$ (see Fig. 1). This plateau has not been observed in previous calculations using NRG.[6] We believe that the reason for this is the lack of resolution of NRG to describe peaks in the spectral density out of the Fermi energy, like that of $\rho_d^s(\omega)$. A clear manifestation of this is a system in which the Kondo peak is split in two out of the Fermi level.[26] In fact, while NRG uses a logarithmic frequency mesh centered at the Fermi energy, we

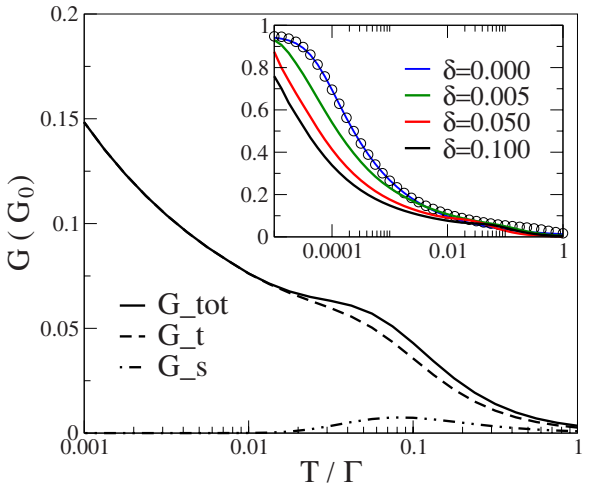

FIG. 3. (Color online) Zero-bias conductance $G(T)$ as a function of temperature (full line) and contributions from the singlet (dashed doted line) and triplet (dashed line) for $E_t=-3, E_s=-2.9$. The inset shows $G(T)$ for $E_t=-3$ and several values of $\delta=E_s-E_t$ (increasing from top to bottom). The circles correspond to Eq. (4). $G_0=2e^2A/h$.

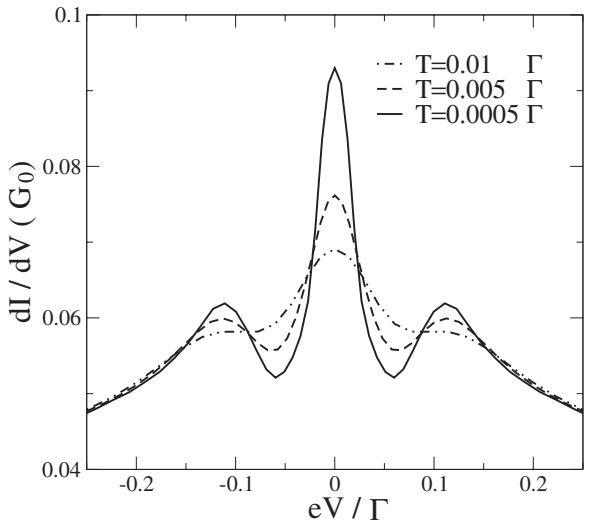

FIG. 4. Differential conductance as a function of bias voltage for $E_t=-3, E_s=-2.9$ and several temperatures.

find that in order to obtain enough accuracy in the convolutions that define $\rho_d^s(\omega)$ and $\rho_d^t(\omega)$, it is necessary to use two different dense logarithmic meshes centered at the corresponding peaks.

The inset of Fig. 3 shows the evolution of the equilibrium conductance as the system is displaced from the quantum critical line to the triplet region. At this line, $G(T)$ is the same as the corresponding result for the OAM obtained using the mapping mentioned above. In this case, a fit of $G(T)$ using the empirical curve is derived by fitting results of the NRG for a spin 1/2

$$G_E(T) = \frac{G(0)}{[1+(2^{1/s}-1)(T/T_K)^2]^s}, \tag{4}$$

with $s=0.22$ works very well. We could not find other regions in which similar empirical curves would fit well to a large portion of the curve. When E_s increases, the degeneracy in the ground state is reduced and $G(T)$ decreases in the whole range of temperatures. However, in contrast to the case $E_s<E_t$, the conductance at zero temperature retains values near to the ideal one $G_0=2e^2A/h$ due to the partial Kondo effect.

In Fig. 4 we show the nonequilibrium differential conductance dI/dV on the triplet side at several temperatures. At low temperatures, there is one peak centered at $V=0$ and other two centered at $V=\pm V_M$. This three-peak structure also agrees qualitatively well with experiment.[2] Actually in the later, the peak at $V=-V_M$ is higher than that at $V=V_M$, while our results are even in V due to our assumption of a symmetric voltage drop. Changing this we can easily control the relative height of both peaks. In any case, the main point is the existence of these three peaks, which is also a consequence of the particular structure of the spectral densities $\rho_d^s(\omega)$ and $\rho_d^t(\omega)$ at equilibrium and low temperatures (see Fig. 1). The peak at $V=0$ is due to $\rho_d^t(\omega)$, which is peaked at the Fermi energy. When $e|V|$ reaches energies at which $\rho_d^s(\omega)$ is peaked, this density starts to contribute significantly to the current I [see Eq. (3)] and dI/dV increases. Finally, for large $e|V|$, I tends to saturate and dI/dV decreases again.

The effect of temperature is to broaden the peaks and at high-enough temperatures only one broad peak in dI/dV is present, in agreement with experiment. For different parameters as those of Fig. 1, this broadening of the spectral densities is already important at $V=T=0$ and increases with $|V|$ in such a way that even at $T=0$ only one peak in dI/dV is present. This happens for example at $E_t=-2\Gamma$ and $E_s-E_t=0.03\Gamma$, for which dI/dV (not shown) has a monotonic behavior for positive V, displaying only a shoulder for $eV \sim \pm(E_s-E_t)$.

In summary, the transport properties recently observed near the singlet-triplet quantum phase transition in quantum dots can be explained in the framework of the singlet-triplet Anderson model with one channel per conduction lead, out of equilibrium, using the noncrossing approximation. We made use of exact results to control the distance to the quantum critical point. The differential conductance dI/dV as a function of bias voltage is markedly different at both sides of the transition showing a dip (peak) at small voltages on the singlet (triplet) side and often a three-peak structure on the triplet side. The zero-bias conductance $G(T)$ as a function of temperature displays a plateau due to the contribution of the excitations from the localized singlet to the doublet.

ACKNOWLEDGMENTS

We thank Ana M. Llois for useful discussions. One of us (A.A.A.) is supported by CONICET. This work was done in the framework of projects under Grants No. PIP 5254 and No. PIP 6016 of CONICET, and under Grants No. PICT 2006/483 and No. 33304 of ANPCyT.

*roura@tandar.cnea.gov.ar

[1] S. Sachdev, *Quantum Phase Transitions* (Cambridge University Press, Cambridge, England, 1999).
[2] N. Roch, S. Florens, V. Bouchiat, W. Wernsdorfer, and F. Balestro, Nature (London) **453**, 633 (2008).
[3] D. Goldhaber-Gordon, H. Shtrikman, D. Mahalu, D. Abusch-Magder, U. Meirav, and M. A. Kastner, Nature (London) **391**, 156 (1998).
[4] W. Liang, M. P. Shores, M. Bockrath, J. R. Long, and H. Park, Nature (London) **417**, 725 (2002).
[5] S. Tarucha, D. G. Austing, Y. Tokura, W. G. van der Wiel, and L. P. Kouwenhoven, Phys. Rev. Lett. **84**, 2485 (2000).
[6] W. Hofstetter and H. Schoeller, Phys. Rev. Lett. **88**, 016803 (2001).
[7] J. Paaske, A. Rosch, P. Wölfle, N. Mason, C. M. Markus, and J. Nygard, Nat. Phys. **2**, 460 (2006).

[8] R. Allub and A. A. Aligia, Phys. Rev. B **52**, 7987 (1995).
[9] S. Sasaki, S. De Franceschi, J. M. Elzerman, W. G. van der Wiel, M. Eto, S. Tarucha, and L. P. Kouwenhoven, Nature (London) **405**, 764 (2000).
[10] J. Schmid, J. Weis, K. Eberl, and K. v. Klitzing, Phys. Rev. Lett. **84**, 5824 (2000).
[11] In the example given in the introduction, they correspond to annihilation of an electron in the lowest electronic level s_σ or in the excited one p_σ, respectively, except for an irrelevant normalization factor.
[12] M. Pustilnik and L. I. Glazman, Phys. Rev. Lett. **87**, 216601 (2001); M. Pustilnik, L. I. Glazman and W. Hofstetter, Phys. Rev. B **68**, 161303(R) (2003); W. Hofstetter and G. Zarand *ibid.* **69**, 235301 (2004).
[13] A. Posazhennikova, B. Bayani, and P. Coleman, Phys. Rev. B **75**, 245329 (2007).
[14] A. A. Aligia, C. A. Balseiro, and C. R. Proetto, Phys. Rev. B **33**, 6476 (1986) and references therein.
[15] A. A. Aligia, Phys. Rev. B **74**, 155125 (2006).
[16] F. B. Anders, Phys. Rev. Lett. **101**, 066804 (2008).
[17] N. S. Wingreen and Y. Meir, Phys. Rev. B **49**, 11040 (1994).
[18] A. C. Hewson, J. Bauer, and A. Oguri, J. Phys.: Condens. Matter **17**, 5413 (2005).
[19] J. Rincón, A. A. Aligia, and K. Hallberg, Phys. Rev. B **79**, 121301(R) (2009).
[20] A. Rosch, J. Paaske, J. Kroha, and P. Wölfle, Phys. Rev. Lett. **90**, 076804 (2003).
[21] P. Roura-Bas, V. Vildosola, and A. M. Llois, Phys. Rev. B **75**, 195129 (2007).
[22] P. Roura-Bas, M. A. Barral, and A. M. Llois, Phys. Rev. B **79**, 075410 (2009).
[23] R. Aguado and D. C. Langreth, Phys. Rev. B **67**, 245307 (2003).
[24] D. L. Cox and A. E. Ruckenstein, Phys. Rev. Lett. **71**, 1613 (1993).
[25] Y. Meir and N. S. Wingreen, Phys. Rev. Lett. **68**, 2512 (1992).
[26] L. Vaugier, A. A. Aligia, and A. M. Lobos, Phys. Rev. B **76**, 165112 (2007).